INTERNATIONAL JOURNAL OF HEAT AND TECHNOLOGY
Vol.33, No.1, 2015

# JET FLOW FIELD CALCULATION & MECHANISM ANALYSIS ON HOT-AIR DRYING OVEN BASED ON RNG K-E MODEL

Linlin Liu [1*], Zhengcheng Sun [2*], Chuliang Wan [3*] and Jimei Wu [4*]

[1,2,3,4*] Institute of Printing and Packing Engineering, Xi' an University of Technology
Xi' an, 710048, Shannxi, China

## ABSTRACT

In order to gain the performance characteristics and technical parameters in drying processing, the paper describes the heat and mass transfer mechanism of solvent which dries and volatilizes during gravure printing, and establishes multi-beam air impinging drying model for suspended hot air drying device; based on standard RNG k-ε model, fluid numerical simulation & calculation are performed for drying oven; the paper extracts hot air fluctuation range and features of velocity on prints surface through sections technique, then discusses the uneven mechanism by combining geometric structure; the research complicates hot air trace in different locations of drying oven; the reasons for turbulence and the influence on drying effect are analyzed. The research on structural characteristics of the impinging jet flow field provides evidence and support to drying system optimization and innovative design.

**Keywords:** drying mechanism, RNG k-ε model, numerical calculation, characteristics analysis.

## 1. INTRODUCTION

The drying system is an important component of a gravure press, which completes forceful drying on prints within a very short time after printing to thoroughly volatilize solvent in liquid state into gas, so as to effectively control remaining solvent on the surface of prints [1]. The drying system is the largest energy-consumption unit of the gravure press whose efficiency is a key factor in restricting velocity of the gravure press and prints quality. The drying technique is an interdisciplinary technique with experimental properties. The structure of the drying device, performances of ink, temperature of hot air and printing velocity in gravure printing will affect drying efficiency, in which, the hot-air dynamics characteristics and structural parameters of drying oven directly affect drying efficiency of the printed products and energy consumption of prints [2].

A lot of researches have done for improving hot-air drying effect of gravure printing and structure of drying oven. Feng Peiyong[3] and Wang Ani [4] have done research on mechanism of hot air drying prints and established the mathematical relationship model between hot air convection drying parameter and remaining solvent; Liu Jian [5] has carried out comparative analysis on different tuyeres of oven and improved the structure; Xu Zonglei [6] has established relationship between hot air output and input parameters of traditional drying oven; Shen Xianwen [7] has identified internal hot air flow state of oven and input/output relationship of hot air, and optimized the oven according to analytic results.

The above research has explained volatilizing and drying process of solvent and internal hot-air flow state of drying oven, which is not persuasive to explain the reasons for complicated flow state and impact to drying. This paper takes hanging drying device of FR400 gravure press as the research object, describes the heat and mass transfer mechanism of the solvent which dries and volatilizes, establishes multi-beam air impinging drying model for suspended hot air drying device. Based on RNG k-ε model, the paper completes hot-air flow field value calculation through fluent and researches hot air flow state and dry characteristics.

## 2. INK DRYING MECHANISM AND DRYING DEVICE

### 2.1 Volatilization and drying mechanism

Gravure ink is composed of pigment, resin, solvent and other components. The volatilization of solvent in the ink demands a great quantity of heat consumption [2]. At present, the drying of high velocity gravure press mostly adopts hot-air convection mode. As shown in Figure 1, high velocity hot air pounds on ink surface directly, transferring the heat to ink, so as to volatilize part of the solvent. Hot air brings volatile and finally makes ink dry completely. The flow path of hot air is short with thin border, leading to comparatively less hot consumption. The drying capacity is several times and even at magnitude level than conduction drying. In addition, it has good and fast drying with less solvent remaining on surface of prints. The drying process belongs to physical and chemical process of heat and mass transfer [3] [4].

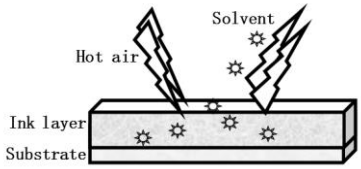


**Figure 1.** Ink drying model

### 2.2. Working principle of hot-air drying system

Structure of the drying device of a gravure printing machine is shown in Figure 2. Firstly, air is heated by the heating tube 11 and the heated air is blown to the drying mechanism 5 by the air blower 8, and then blown on surfaces of the substrate 4 by the air tuyere 3, and finally exhausted by the air exhausting duct 2 [2]. Parts of hot air enter the secondary circulation loop to realize secondary utilization of thermal energy.

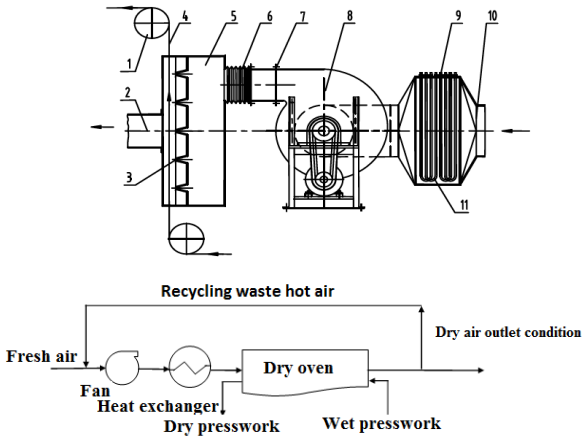


**Figure 2.** Hot air drying system model

The paper establishes simulation model based on drying oven of FR400 gravure press. As shown in Figure 3, deflector guides hot air in inlet to chambers at top and bottom. The lowest tuyere is tuyere 1. All tuyeres are ranked from bottom up till tuyere 13. The hot air is jetted out in a long and narrow tuyere by pressure difference and forms high velocity air flow from free jetting area. Which is pounded on the membrane at a certain distance from the gap of tuyere vertically (or inclined), which model is as shown in Figure 3.

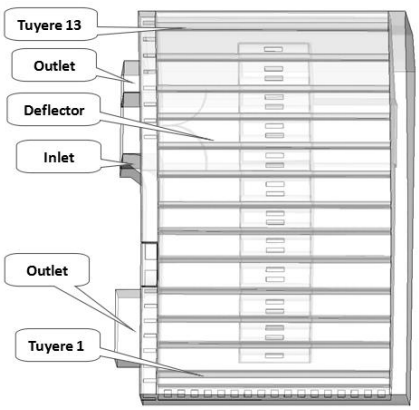


**Figure 3.** Suspended drying oven model

As shown in figure 4, since there are rows of tuyeres, jets between tuyeres interfere with each other, which is the multi-beam air impinging jet drying. After forming stable flow, hot air scatters on the plane which forms wall jet area and hot air stagnation in the middle. In a very small transitional area (the length is related to Reynolds coefficient) close to the tuyere, high-velocity jet flow causes a shear layer, which instability grows rapidly and forms vortex with surrounding flow. It is closely related to hot air loss and solvent steaming and flowing velocity, which further affects the drying velocity[5][8].

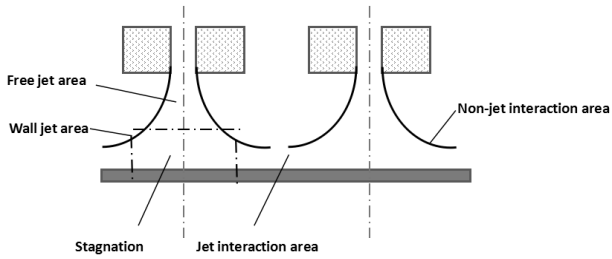


**Figure 4.** Multi-beam air impinging jet drying model

## 3. FLUID NUMERICAL SIMULATION

### 3.1 CFD simulation model

Under control of the basic control equations for fluid flow (mass conservation equation, momentum conservation equation and energy conservation equation), flow states of the fluid can be analyzed through numerical simulation to obtain the flow field in the fluid domain and distribution of hot air on a continuous area, so as to approximately simulate the situation of hot air flow and to implement optimal design on the structure according to the analysis results [5]. This research regards air flow of drying oven as turbulence flow of incompressible 3D air and analyzes values of flow velocity, temperature and evenness of drying oven through fluent.

Due to complexity of hot air fluid domain inside the drying device, Boolean operation should be carried out on the whole drying device to distinguish all areas of hot air flow [6]. Therefore, it should be assumed that the drying device is closed, the fluid domain of hot air is only limited inside the drying device and no loss of air velocity and air pressure is considered; errors of fabrication and assembly should be neglected and deformation problems of the drying device caused by fabrication precision and installation should be neglected [7].

The hot air in the drying device belongs to constant viscous fluid. The Reynolds number is calculated to determine flow states of hot air in the drying system [8] [9].

$$Re = \rho \frac{VL}{\nu} \tag{1}$$

Where V refers to average velocity at the section, L refers to length; v refers to moving viscosity of fluid. The Reynolds number of hot air in inlet of FR400 drying oven model is 352,130 [10], greater than the critical Reynolds number of 4,620, so it is turbulent flow and the turbulent flow RNG k-ε model should be used for simulation calculation [11].

To simplify the question, the following assumptions are made:

(1) The fluid domain within the hot air flow area is a constant;
(2) The flow of hot air inside the drying device is steady turbulent flow;
(3) The flow process of hot air in the whole fluid domain is steady flow [12];
(4) Flow velocity of air at inlet of the air tuyeres is uniform and is average value of the total flow quantity [13] [14].

### 3.2 Boundary conditions

(1) Wall boundary conditions and physical properties

Set the wall of drying cabinet with heat insulation but no slippery, adopt standard wall function, and give the surface roughness of 0.005m according to wall quality of drying cabinet, then the air density is $\rho = 1.205\,\mathrm{kg/m^3}$, viscosity coefficient is $\mu = 1.7894e-05\,\mathrm{Pa\cdot s}$, specific heat is $Cp = 1006.43\,\mathrm{J/kg\cdot K}$ and thermal conductivity is $\varepsilon = 0.0242\,\mathrm{W/m\cdot K}$ [15].

(2) Boundary conditions on hot air inlet

The turbulence strength and dissipation rate is identified as $k$ =0.391, $\varepsilon$ =1.86 according to hydrodynamics. The fan velocity is 2232r/min, pressure in inlet is 3,929Pa, and temperature in inlet is 360K. When the referential pressure is 0Pa, the production techniques shall ensure external pressure of chamber of drying cabinet between -10Pa to 20Pa, while the outlet pressure should be adjusted accordingly [16].

(3) Choose solution method and control parameters

This paper chooses 3D single precise segregated solver based on flowing properties of hot air in drying oven and steady 3D flow, and adopts implicit method to linearize dissipated nonlinear control equation, so as to calculate equation set of related variable in each calculation unit and solve each equation (about $u, v, w, p \& T$) one by one in sequence[17] [18].

Choose SIMPLE as the solving method of control equation and two-phase discrete pattern, set pressure under-relaxation factor coefficient to 0.3, energy under-relaxation factor coefficient to 0.8, and others to default value. The convergence standard of monitoring parameters is the motion control equation while the iterative residue of dynamics control equation is approximately $1\times10^{-3}$ and iterative residue of energy control equation is approximately $1\times10^{-6}$ [19] [20].

## 4. HOT AIR VELOCITY IN DRYING OVEN

### 4.1 Hot air velocity field

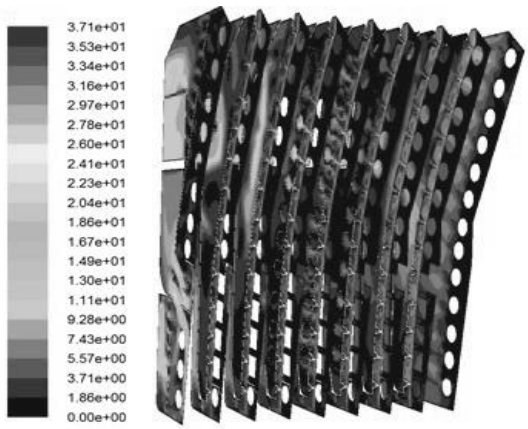


**Figure 5.** Hot air velocity nephogram

Analyze characteristics of hot air drying system specifically and cut 9 sections with equal distance along the direction vertical to tuyere. As shown in Figure5, it is the hot air velocity nephogram of the section, which indicates that it flows faster in the intersection between tuyere and inlet and inlet channel, it flows slowest in the back of returning air chamber, and the oven returns air from the right of return air chamber.

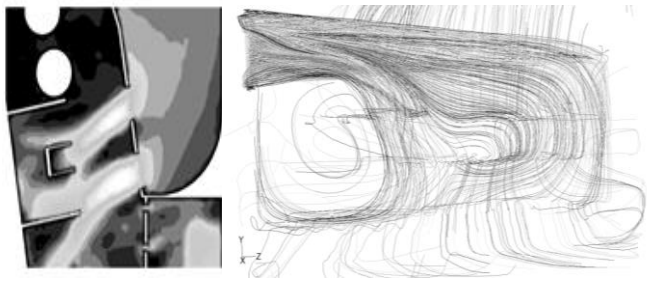

**Figure 6.** Velocity nephogram of the back

The Figure 6 shows the velocity nephogram of the back inlet channel, which indicates that hot air in back inlet channel mostly blows inclined downward and doesn't enters back blowing chamber, leading to energy loss.

**Table 1.** Hot air velocity in different locations (Unit: m/s)

| Section | 1 | 2 | 3 | 4 | 5 | 6 | 7 | Average velocity | Horizontal variance |
|---|---|---|---|---|---|---|---|---|---|
| Tuyere1 | 23.643 | 24.145 | 26.543 | 21.649 | 25.510 | 20.743 | 24.853 | 23.869 | 4.273 |
| Tuyere2 | 22.109 | 24.455 | 27.498 | 25.517 | 24.745 | 26.823 | 24.406 | 25.079 | 3.144 |
| Tuyere3 | 25.850 | 21.975 | 24.687 | 26.251 | 24.348 | 24.261 | 27.575 | 24.992 | 3.189 |
| Tuyere4 | 25.586 | 25.257 | 25.395 | 26.206 | 25.539 | 25.996 | 26.654 | 25.805 | 0.251 |
| Tuyere5 | 24.528 | 26.331 | 24.720 | 25.759 | 23.991 | 26.255 | 26.123 | 25.387 | 0.909 |
| Tuyere6 | 28.511 | 27.115 | 26.255 | 25.834 | 22.416 | 27.459 | 27.846 | 26.491 | 4.056 |
| Tuyere7 | 25.078 | 25.128 | 24.074 | 22.115 | 24.088 | 23.394 | 25.414 | 24.184 | 1.355 |
| Tuyere8 | 22.904 | 26.413 | 24.393 | 25.362 | 23.855 | 26.141 | 25.979 | 25.006 | 1.744 |
| Tuyere9 | 25.884 | 27.629 | 25.693 | 26.371 | 25.596 | 27.215 | 24.405 | 26.113 | 1.165 |
| Tuyere10 | 25.743 | 23.880 | 24.889 | 25.912 | 24.780 | 25.494 | 22.842 | 24.791 | 1.216 |
| Tuyere11 | 24.120 | 25.147 | 23.246 | 23.727 | 25.495 | 25.538 | 27.233 | 24.929 | 1.829 |
| Tuyere12 | 24.462 | 24.229 | 25.668 | 24.636 | 26.796 | 25.293 | 25.413 | 25.214 | 0.771 |
| Tuyere13 | 24.278 | 24.435 | 24.654 | 27.631 | 23.497 | 26.879 | 24.939 | 25.188 | 2.238 |
| Average velocity | 24.823 | 25.087 | 25.209 | 25.151 | 24.666 | 25.499 | 25.668 | | |
| Vertical variance | 2.561 | 2.292 | 1.277 | 2.944 | 1.297 | 3.358 | 2.050 | | |

In order to analyze flow state within drying oven straightforwardly, analyze hot air velocity, temperature and other parameters on surface of substrate in quantitative manner, the paper chooses 7 slices in the tuyere region as figure 5 to represent different locations on the substrate and extract fluid value at the 12mm vertical to outlet of tuyere as the drying parameters for surface of substrate, as shown in Table 1. It shows hot air velocity at different location of sections of the substrate, which indicates that air coming out from tuyere by 20.743m/s～28.511m/s. The largest velocity difference in different location is 7.768m/s, the largest difference of average velocity in each tuyere is 1.207m/s, and the average velocity is 24.158m/s.

### 4.2 Horizontal velocity fluctuation

Analyze air velocity in different tuyeres and paint the change curve of velocity along horizontal direction, which is as shown in Figure 7, to present change and uniformity of horizontal outlet velocity.

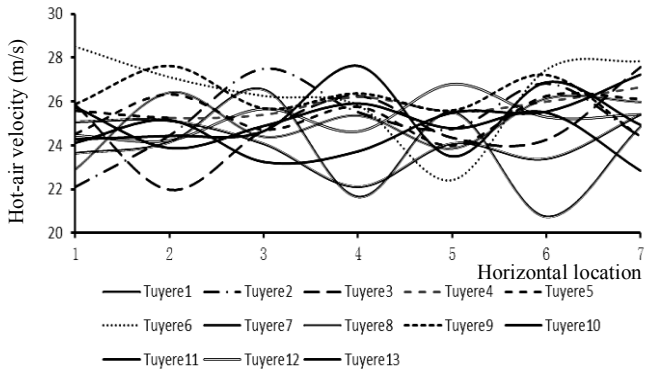


**Figure 7.** Velocity curve of tuyere along horizontal positions

The minimal variable of slice 3 is 1.277, the maximal variance of slice 6 is 3.358, indicating that fluctuation at slice 3 of the substrate is the smallest while that at slice 6 is the greatest. In regard of drying capacity or drying effect at different regions with different average air velocity characteristics, the drying effect is the worst in the far left position (slice 1) and right to the middle (slice 5) of prints while the effect is the best in the far right position.

Analyze the relationship between geometric structure and hot air velocity in drying system from the granularity according to geometric structure of drying oven. Hot air going downward in left and right chambers enters tuyere 1 and 2 after collision with the wall and interacts with each other, showing sinusoid fluctuation and less uniform velocity. Air in tuyere 3 and 4 comes from hot air at two sides of turbulence in right and left chambers, which is symmetric and shows w-shape distribution. Affected by the location, air velocity in tuyere 3 is not uniform enough while air velocity in tuyere 4 is quite uniform. Tuyere 6 is located at the intersection of two turbulences with obvious interference; in the right of round pipe shows slower air velocity but obvious fluctuation; tuyere 5 and 7 at two sides shows stable air velocity; tuyere 8, 9, 10, 11 and 12 has stable air velocity because inlet air in the left chamber is influenced by deflector, among which tuyere 10 is at the center of two deflectors; tuyere 13 is at the top of drying oven, which left and right chambers have received impact of turbulence at the top, showing sinusoidal fluctuation with worse uniformity.

### 4.3 Lengthways velocity fluctuation

Prints go through tuyere 1 to 13 in turn. Paint hot air velocity change curve if we set location of tuyere equivalent to time course of prints within the drying oven. Define tuyere 1 to 3 as the pre-drying stage, tuyere 4 to 10 as the constant drying stage, and tuyere 11 to 13 as the decelerated drying stage. Figure 8 shows air velocity change in different drying stages in different regions of prints.

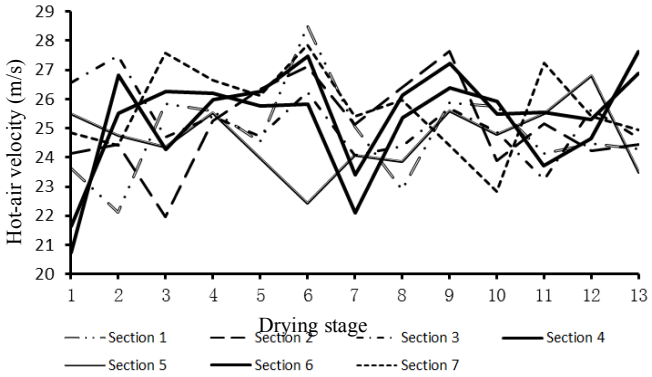


**Figure 8.** Velocity curve of tuyere along time

As shown in Figure 8, air velocity in symmetric positions in the left and right chambers shows similar trend. Left and right regions of prints shown in slice 1 and 7 are affected by the side wall and show V-shape fluctuation in pre-drying stage after entering the oven.

The fluctuation is more serious in constant drying stage, the air velocity is higher in medium stage (at tuyere 6), and air velocity is more stable in decelerated drying stage; in regions shown in slice 2 and 6, hot air shows greater fluctuation in pre-drying stage after entering the oven, and M-shape fluctuation in constant drying stage, lower velocity in medium stage (at tuyere 7) and stable velocity in decelerated drying stage; in the medium region of substrate shown in slice 3 and 4 is affected by round pipe in the middle, which hot air fluctuates greatly in pre-drying stage after entering the oven, shows flat fluctuation in constant drying stage, and lower velocity in medium stage with constant drying (at tuyere 6 and 7), but greater fluctuation in decelerated drying stage.

## 5. HOT-AIR FLOW STATE OF DRYING OVEN

As shown in Figure 9, flowing trace of single mass point within a continuous process is a method of Lagrange to describe flowing. The flow state of hot air in drying oven can be mastered intuitively through analysis on overall and local flow trace of drying oven.

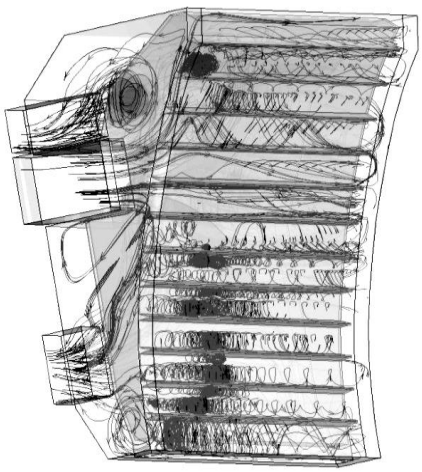

**Figure 9.** Trace map of drying oven

Firstly, hot air goes in drying oven and forms turbulence on two ends of deflector in left chamber and upper right chamber because of change of channel section and interaction of hot air and oven.

The asymmetric pressure distribution in the front and at the back causes greater pressure drag and generates boundary separation. The ongoing hot air changes the direction after meeting deflector and forms turbulence in left chamber through interaction with the wall.

Hot air enters right chamber of drying oven through the channel. A small part of hot air goes right and large quantity of hot air moves forward from the back of drying oven, leading to collision of hot air from two different directions and collision of hot air and wall. In addition, the inlet is close to upper right of the chamber, which space is comparatively small; therefore, turbulence is generated here in right chamber. Secondly, the trace map shows clearly that there are more hot air flow in the round pipe in inlet because of influence of different air intake methods in the left and right chambers. Hot air in the round pipe enters through right chamber, so the flow is less.

Figure 9 indicates that vortex forms between two tuyeres mainly by return air from the right of drying oven (far from the outlet). The return air in the right moves to the right in the form of whirl. Hot air from tuyere 9 to 13 is discharged by upper tuyeres and the hot air of rest tuyeres is discharged by lower tuyeres. Most hot air is pumped by lower outlets, effectively increasing the time for substrate to contact with hot air, so as to achieve better drying effect.

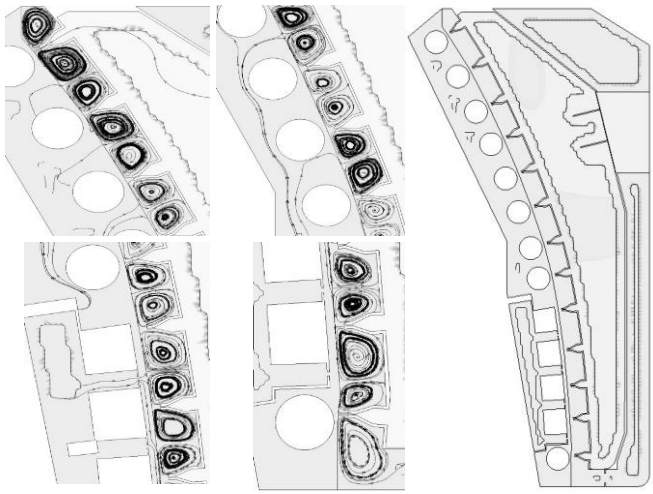

**Figure 10.** Trace section of tuyere

Extract trace section along direction vertical to tuyere, as shown in Figure 10. Hot air returns at two sides after reaching prints. Vortex region forms between two return regions in nearby tuyeres. The size and shape of vortex region is affected by location of tuyeres, distribution distance, structure and size of tuyere, which distributes in interval. The generation of vortex region can expand the drying region of ink and accelerate energy exchange on surface of paper, which is conducive to ink drying.

Extract trace section at corresponding connecting round pipe along direction vertical to tuyere, as shown in Figure 11. Hot air between tuyere 1 to 6 is pumped by lower outlet at the orifice plate and forms small vortex at the bottom, which is easy to cause deposition of solvent in hot air. Hot air between tuyere 6 to 13 is pumped by upper outlet and forms greater vortex at the top of drying oven, which causes deposition and gathering of solvent in hot air. Therefore, upper outlet shall be set below the vortex region.

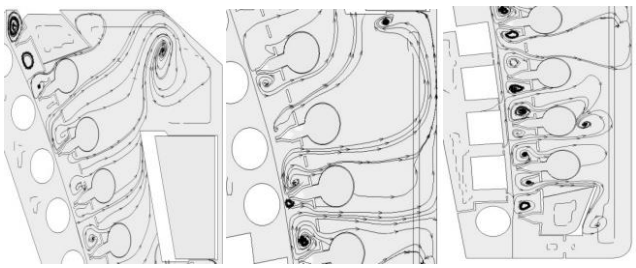

**Figure 11.** Trace section of connecting pipe

## 6. CONCLUSION

Taking hanging drying device of FR400 gravure press as the research object, the paper researches hot-air velocity field in key positions and hot-air flow state based on structure of drying oven to provide evidence for structure improvement and innovative design for drying system.

The major conclusion is as follows:

(l) Hot air impinging substrate is in line with multi-beam impinging jet drying model and hot air drying system is in line with RNG k-ɛturbulence model, based on which CFD hot air simulation model is established.

(2) The hot air velocity on surface of prints fluctuates between 20.743m/s to 28.511m/s, which are more even in tuyere in the middle and worse at upper and lower sides; the drying process of prints is different in different regions, with worse effect in left region. Therefore, try to reduce text and picture allocation in the left.

(3) Turbulence is generated on two sides of deflector in left chamber and upper right chamber of drying oven and vortex region is formed between tuyeres in interval, which is conducive to ink drying; drying oven gets returned air by the right side, therefore, it should adopt tuyeres at upper and lower rows; considering solvent gathering, the upper returned air shall be set in lower vortex region.

## ACKNOWLEDGMENTS

The author gratefully acknowledges the support of the National Natural Science Foundation of China (Grant No. 11272253), China Postdoctoral Science Foundation (2014M552484), Natural Science Foundation of Shaanxi Province (2014JM8334), Science Foundation of Shaanxi Educational Department (Natural Science 2013jk0996), and Science Foundation of Xi'an University of Technology (104-211106).

## REFERENCES

1. Jiangyan Bei, *Gravure Printing*, Chemical Industry Press, 2008.
2. Weili Wang, Wenge Chen, "The analysis on drying system of gravure press", *Journal of Packaging Engineer*ing, Vol.6, pp.98-100, 2008.
3. Peiyong Feng, *Parmeter optimization of dry System of plastic gravure printing machine*, Xi'an University of Technology, 2006.
4. Ani Wang, *Parmeter optimization of plastic gravure printing machine hot air drying*, Xi'an University of Technology, 2008.
5. Jian Liu, *Analysis and structure optimization of hot air drying device in a gravure printing machine*, Xi'an University of Technology, 2011.
6. Zonglei Xu, *Analysis of fluid dynamic characteristic analysis and parameter optimization of drying mechanism in a gravure printing machine*, Xi'an University of Technology, 2011.
7. Xianwen Shen, *The Hot-air Fluid Dynamic Analysis and Structure optimization of the YF93 Oven for the Gravure printing machines*, Xi'an University of Technology, 2013.
8. Qingming Huang, Fang-yuan Chen, Neng-sheng Bao, Peng Xu, Wen-hua Bai, "Research and design for temperature optimized control system of drying oven to gravure press", *Journal of Manufacturing Informatization*, Vol.13, pp.68-72, 2008.
9. Jing Wang, *Basis of Heat Transfer and Fluid Dynamics*, Shanghai Jiaotong University Press, 2007.
10. Hongli Liu, Tao Meng, *Fluid Dynamics: Pump and Air Blower*, China Electric Power Press, 2008.
11. Autel, *Basis of Prandtl Fluid Dynamics*, Science Press, 2008.
12. Best Practice Guidelines, *Version 1.0, ERCOFTAC Special Interest Group on "Quality and Trust in Industrial CFD"*, January, 2000.
13. Ren Yuxin, *Basis of Computational Fluid Dynamics*, Tsinghua University Press, 2006.
14. Lindfield G, Penny J, *Numerical Methods Using MATLAB*, 2nd, Prentice Hall, 2006.
15. Jin Yinhe, *Flexography Printing*, Chemical Industry Press, 2001.
16. Song Hui, Pan Ying, "Application of far infrared radiation and hot air convection drying", *China Bicycle*, Vol.3, pp.23-25, 1996.
17. Yang Xuefeng, Zhang Yan, "Fluid flow in FHP-2 lattice gas model simulation pipeline", *Journal of Fushun Petroleum Insti*tute, Vol.16, No.1, pp.43-46, 2000.
18. Bruno Eck. Fans, *Design and Operation of Centrifugal, Axial-Flow and cross-Flow Fans*, Pergamon Press LTD, 1973.
19. S.Kakac, A.E.Bergles, F.Mayinger, *Heat Exchangers-Thermal-Hydraulic Fundamentals and Design*, McGraw-Hill, 1980.
20. Anderson J.D, *Computational Fluid Dynamics: the basics with applications*, McGraw-Hill, 1995.